The Breast 45 (2019) 64–69

Contents lists available at ScienceDirect

The Breast

journal homepage: www.elsevier.com/brst

Original article

Towards mm-wave spectroscopy for dielectric characterization of breast surgical margins

Paul E. Summers [a, *], Andrea Vingiani [b], Salvatore Di Pietro [c], Andrea Martellosio [a, d], Pedro F. Espin-Lopez [a, d], Simona Di Meo [d], Marco Pasian [d], Michele Ghitti [e, 1], Marco Mangiacotti [e], Roberto Sacchi [e], Paolo Veronesi [f], Maurizio Bozzi [d], Andrea Mazzanti [d], Luca Perregrini [d], Francesco Svelto [d], Lorenzo Preda [a, 2, 3], Massimo Bellomi [a, g], Giuseppe Renne [b]

[a] Division of Radiology, IEO, European Institute of Oncology IRCCS, Milan, Italy
[b] Division of Pathology, IEO, European Institute of Oncology IRCCS, Milan, Italy
[c] Post-graduate School of Radiodiagnostics, University of Milan, Milan, Italy
[d] Department of Electrical, Computer and Biomedical Engineering, University of Pavia, Pavia, Italy
[e] Applied Statistics Unit, Department of Earth and Environmental Sciences, University of Pavia, Pavia, Italy
[f] Division of Senology, IEO, European Institute of Oncology IRCCS, Milan, Italy
[g] Department of Oncology and Hemato-Oncology, University of Milan, Milan, Italy

ARTICLE INFO

Article history:
Received 30 October 2018
Received in revised form
17 January 2019
Accepted 19 February 2019
Available online 27 February 2019

Keywords:
Surgical margin
Tissue discrimination
Millimeter waves
Dielectric tissue properties

ABSTRACT

Purpose: The evaluation of the surgical margin in breast conservative surgery is a matter of general interest as such treatments are subject to the critical issue of margin status as positive surgical margins can undermine the effectiveness of the procedure. The relatively unexplored ability of millimeter-wave (mm-wave) spectroscopy to provide insight into the dielectric properties of breast tissues was investigated as a precursor to their possible use in assessment of surgical margins.

Methods: We assessed the ability of a mm-wave system with a roughly hemispherical sensitive volume of ~3 mm radius to distinguish malignant breast lesions in prospectively and consecutively collected tumoral and non-tumoral ex-vivo breast tissue samples from 91 patients. We characterized the dielectric properties of 346 sites in these samples, encompassing malignant, fibrocystic disease and normal breast tissues. An expert pathologist subsequently evaluated all measurement sites.

Results: At multivariate analysis, mm-wave dielectric properties were significantly correlated to histologic diagnosis and fat content. Further, using 5-fold cross-validation in a Bayesian logistic mixed model that considered the patient as a random effect, the mm-wave dielectric properties of neoplastic tissues were significantly different from normal breast tissues, but not from fibrocystic tissue.

Conclusion: Reliable discrimination of malignant from normal, fat-rich breast tissue to a depth compatible with surgical margin assessment requirements was achieved with mm-wave spectroscopy.

1. Introduction

Breast-conserving surgical management of breast cancer relies on quadrantectomy, lumpectomy and, more recently, on nipple sparing mastectomy [1,2]. Assuring the cancer is contained within the resected tissue requires a margin of healthy tissue between the outer limit of the tumor and the resection surface. Negative surgical margins are significantly correlated with lower rates of local recurrence [3,4] while positive margins have the potential to undermine procedure effectiveness. For ductal carcinoma in situ, it

Abbreviations: mm-wave, millimeter wave; NBT, normal breast tissue; FCD, fibrocystic disease; MAL, malignant.

* Corresponding author. Division of Radiology, IEO European Institute of Oncology IRCCS, via Giuseppe Ripamonti 435, 20141 Milan, Italy.
E-mail address: paul.summers@ieo.it (P.E. Summers).
[1] Present Address: Customer Analytics and Big Data Group, UBI Banca, Bergamo, Italy.
[2] Present Address: Department of Clinical-Surgical, Diagnostic and Pediatric Sciences, University of Pavia, Pavia, Italy.
[3] Present Address: Diagnostic Imaging Unit, National Center of Oncological Hadron Therapy (CNAO), Pavia, Italy.

https://doi.org/10.1016/j.breast.2019.02.008
0960-9776/

has been estimated that breast-conserving surgical procedures with a clear margin of 2 mm or more can be reliably considered as radical, while narrower margins are associated with progressively increasing local recurrence [5,6]. In this context, it has been estimated that 20–25% of breast cancer patients undergo re-excision due to positive or close (<2 mm) surgical margins, with consequent patient discomfort and increased costs [7–9].

A common strategy for minimizing the risk of positive surgical margins is intraoperative macroscopic assessment by a pathologist, with or without a frozen section examination of the resection margins closest to the neoplasm. Unfortunately, this requires the availability of a pathologist, increases pathology workload, and has high direct and indirect costs, stimulating research for alternative margin assessment strategies.

Several devices for intraoperative surgical margin assessment have arrived on the market, drawing on a range of operating principles, including destructive rapid evaporative ionization mass spectrometry (e.g. iKnife®, Waters Corporation, USA) [10]. Differences between the interactions of electromagnetic fields with malignant and normal tissues that have been observed over a broad range of frequencies [11,12] form the basis for margin assessment based on non-destructive dielectric spectroscopy at low frequency (e.g. ClearEdge®, LS Biopath, USA) [13], radio (e.g. Marginprobe®, Dune Medical Devices, USA) [14–17] or terahertz frequencies (e.g. TPS Spectra3000®, Teraview Ltd., UK) [18]. In addition, several techniques have been demonstrated to have potential in this role. These include conventional radiological techniques such as x-ray and optical computed tomography [19,20], ultrasound [21] and magnetic resonance [22], as well as adaptations of microscopy [23–25] and various applications of spectroscopy [26–28] and fluorescence imaging [29]. Recently, combinations of techniques [30] and the emerging methods such tissue elastography and photo-acoustics [31,32] have been introduced, while work continues on the strategy of tumor-specific fluorescent dyes [33].

For technological reasons, relatively little attention has been given to electromagnetic interactions at frequencies between 10 and 150 GHz (referred to as millimeter waves, or mm-waves). Relative to radio and microwaves, the shorter wavelength of mm-waves is of considerable interest for imaging systems because they should permit higher spatial resolution, while having greater penetration depths than higher frequency terahertz waves [34,35]. The penetration by mm-waves to depths of a few millimetres in human tissues with simple antennas may likewise present an interesting option for surgical margin testing.

In order to assess the ability of mm-waves to distinguish malignant breast lesions from surrounding breast tissues, we tested a mm-wave spectroscopy system on prospectively and consecutively collected tumoral and non-tumoral ex-vivo breast tissue samples.

2. Materials and methods

Women undergoing breast cancer surgery were candidates for this ethics committee-approved study. All participants provided informed consent for measurements of dielectric tissue properties to be performed on the breast tissue excised in the course of their surgery.

2.1. Preparation of tissue samples

Immediately following excision, fresh specimens were delivered to the gross pathology room for standard gross examination. Between 1 and 3 (median and mode 1) parallelepipeds of tissue (7–10 mm width and height, 7–35 mm length), including breast lesions and healthy tissue, were isolated and shaped for measurement within a target of 90 min of excision. If not handled immediately, the fresh specimen was maintained in a vacuum bag at a temperature of 4 °C.

2.2. mm-wave measurements

The system and procedures used for dielectric property measurements have been previously described [36,37]. In brief, it consists of a computer-controlled vector network analyzer (VNA) (E8361C, Keysight Technologies Italia, Milan, Italy) connected by a cable to a sealed coaxial antenna probe (Dielectric probe kit 85070E, Keysight Technologies Italia, Milan, Italy). The sensitivity of the probe tapers with depth and distance from axis of the probe [37], forming a roughly hemispherical sensitive volume of ~3 mm radius (Fig. 1), thus providing a close approximation of the needs of surgical margin assessment where a margin can be considered "clean" if tumor cells are not present to a depth of 2 mm.

Dielectric property measurements were then performed on 1 to 5 (median and mode 3) neighboring sites roughly 8 mm apart on each tissue sample. With the tip of the probe placed in contact with the tissue sample at a slight contact force, the VNA measured the dielectric properties at 1000 frequencies linearly spaced over the range from 0.5 to 50 GHz, and a computer recorded these values. The measurement was repeated five times for each site and averaged. The individual measurement sites were then inked to facilitate localization at histopathology (Fig. 1a).

2.3. Histopathology evaluation

Full-face histology slides similar to those used for clinical histological margin evaluation (i.e. orthogonal to the cutting surface; Fig. 1b) were subsequently obtained oriented perpendicular to the surface of contact with the mm-wave probe on a mid-plane of the sensitive volumes. A pathologist with 20 years experience in breast

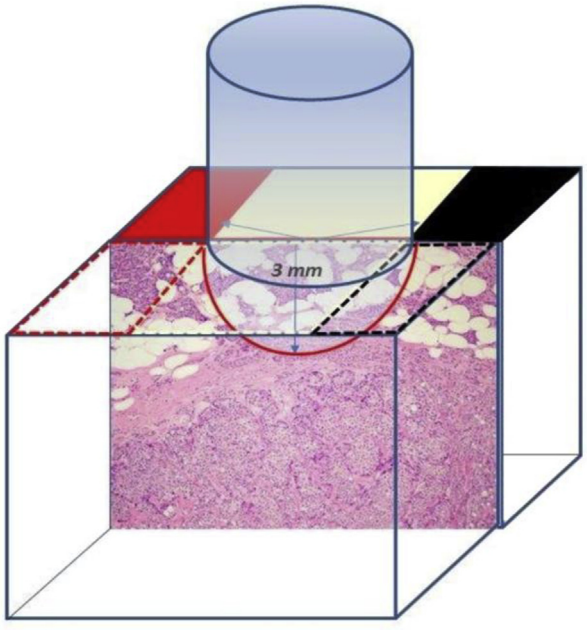

Fig. 1. Each parallelepiped tissue sample was placed in contact with the mm-wave probe (grey cylinder) and dielectric property measures performed over the 0.5–50 GHz range. One to five sites were subjected to measurement on each parallelepiped and then inked with a distinct color (shown here as red, yellow and black). After fixation, full-face histology slides (inset) were prepared perpendicular to the surface of measurement and passing through the centers of the inked regions.

tissue histopathology assessed the slide for the presence of breast lesions and measured the distance of any identified lesion from the surface in contact with the mm-wave probe.

For each measurement site, breast tissue contained within the estimated sensitive volume of the mm-wave probe was histologically assessed and classified into three categories: normal breast tissue (NBT), fibrocystic disease (FCD), and malignant (MAL). The MAL category encompassed both invasive and non-invasive lesions, as both are grounds for resection widening by the surgeon.

Clinical measurement and pathological parameters recorded for their possible influence on the measurements were: age, menopausal status (pre-post-), time to measurement after surgery, probe-lesion distance in μm as seen at pathology (binarized as direct contact/no contact), cellularity, histologic aspect (variegated versus homogenous), percentages of adipose, and of fibrous or epithelial tissues. In case of malignant lesions, pathological characteristics recorded included tumor size, grade, istotype, growth pattern classification [38], nodal status, and immunohistochemical expression of estrogen receptors, progesterone receptors, HER2/NEU and Ki-67 labeling index, but are not examined in the statistical analysis herein.

The data acquired for each measurement site were fitted (Matlab 2016, Mathworks, Natick USA) to a single-pole formulation of the Cole-Cole model for dielectric permittivity [12] to obtain 5 parameters: e_s, e_∞ (the tissue permittivity at extremely low and high frequencies respectively); σ_s (the tissue conductivity); τ (a relaxation time for recovery from changes to the electric field in the tissue); and α (a fitting term describing the dependence of permittivity on change in frequency). Fitting quality was assessed by residual errors to ensure that all results were physically plausible.

2.4. Statistical analysis

Statistical analyses were carried out using R software (ver. 3.3, R Foundation for Statistical Computing, Vienna, Austria) [39]. In preparation for the evaluation of diagnostic performance, we first evaluated whether, and which Cole-Cole parameters vary with diagnosis, tissue characteristics, and patient demographics, by Bayesian multivariate generalized linear mixed models with Gaussian error distribution using the MCMCglmm package in R [40]. The patients were considered a random effect as multiple sites were measured in each patient.

Reflecting the clinical priority of ensuring malignant sites are recognized, we subsequently, assessed the capability of Cole-Cole parameters to classify samples as malignant (MAL) vs non-malignant (NBT + FCD). In consideration of the findings in the random effects analysis, the classification was conducted with a Bayesian logistic model (MCMCglmm with binomial error distribution), considering the patient as a random effect. The output variable in this approach is the probability that a sample is malignant. The logistic model was validated using cross-folding: the set of samples was divided at random into 5 equal-sized subsets, each having the same distribution of malignant/healthy samples; and in turns, 4 subsets were used for generation of the model and the fifth used for testing. A receiver operator curve (ROC) assessment was performed to evaluate the overall ability of the model to correctly identify MAL relative to the other two groups. Additional ROC assessments of classification performance were carried out for the distinction between pairs of subgroups: MAL vs NBT, FCD vs NBT, and MAL vs FCD.

3. Results

124 female patients who had been scheduled for breast surgery were recruited to this study. In 26 cases, the time between excision and initiation of gross pathology preparation exceeded the maximum time post-excision of 4 h, and in seven the tissue samples were too small and did not proceed to measurement. In the remaining 91 patients, dielectric properties and histopathology were obtained for 346 breast tissue sites, encompassing a broad spectrum of the most common breast lesions. A summary of patient, and tumor characteristics is given in Table 1.

We consider the mixed model analysis outputs in three parts: the fixed effects associated with possible explanatory variables, a random effect associated with the patients themselves, and the fixed effect of interest, classification according to histological category. Only two Cole-Cole parameters, namely e_s and σ_s, were seen to be significantly correlated with histologic aspect ($p < 0.05$) and fat content ($p < 0.001$) (Fig. 3 left panel and Supplementary Table 1). None of the Cole-Cole parameters were significantly associated with the other explanatory variables tested (menopausal status, cellularity, percentage of fibrous or epithelial tissues or the probe-lesion distance (see Supplementary Figure 1).

Notably, the random effect of individual patients was associated with significant variability in the Cole-Cole parameters between patients (random effect: $p < 0.001$) that was not strictly related to histopathological classification (see Supplementary Figure 2) and accounted for between 3.4% and 11.9% of the total variance in the parameters. The Cole-Cole parameter τ was the least affected by patient.

Finally, the fixed effect for histopatholocal classification (Fig. 2) showed the MAL samples to have Cole-Cole coefficients significantly different from those associated with NBT ($p = 0.006$), but not significantly different from FCD ($p = 0.064$).

The logistic model showed that Cole-Cole parameters could reliably (AUC $= 0.78 \pm 0.03$) distinguish malignant (MAL) from benign (NBT + FCD) tissues (Fig. 3a, Table 2), with high sensitivity (0.869) and moderate specificity (0.574), corresponding to a low false negative rate (0.131) and moderate false positive rate (0.426); with the false positives being dominated by fibrocystic tissues.

The classification of pairs of subgroups fully supported these

Table 1
Summary of patient demographics, and sample characteristics.

Characteristic	Patients	Tissue Subgroups		
		NBT	FC	MAL
Patients (#)	91			
Age (mean (range))	53.8 (28–80)yrs			
Post-Menopausal (#, (%))	37 (40.9%)			
Time Post-Excision[a] (mean (range))	85 (10–228)min			
Measurement Sites (#)	346	97	142	107
Fat Content (mean (s.d))		94.7 (0.8%)	28.7 (2.6%)	10.1 (1.8%)
Direct Contact (#, (%))		85 (87.6%)	121 (85.2%)	83 (77.6%)

[a] If not examined within 20 min, the samples were stored in vacuum bags at 4 °C, maximum allowed time post-excision was 4 h.

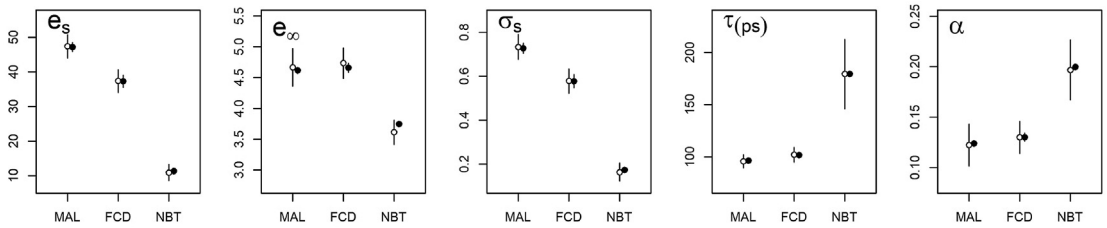

Fig. 2. Results for fixed effect associated with histological classification fitted by the Bayesian multivariate generalized linear mixed (MCMCglmm). The observed means and standard deviations (white circles and bars) of Cole-Cole parameters (from left to right: e_s, e_∞, σ, τ and α) along with their fitted model values (filled circles) in malignant (MAL, n = 107), fibrocystic disease (FCD, n = 142), and normal breast tissues (NBT, n = 97). Clear distinction is seen between MAL samples and NBT (p = 0.006), but MAL were not significantly different from FCD (p = 0.064).

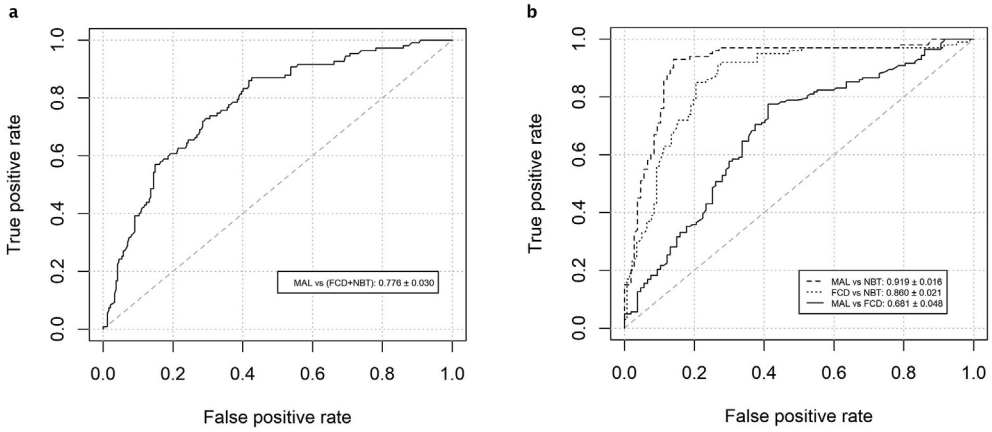

Fig. 3. a) The overall differentiation between malignant (MAL) and non-malignant (FCD + NBT) tissues gave an AUC of 0.78. b) Comparing ROC curves for tissue subgroups; differentiation between MAL and the FCD subgroup had an AUC of 0.92 (dashed line) while between MAL and FCD the AUC was 0.68 (solid line). The differentiation between FCD and NBT was intermediate between the others, with an AUC of 0.86.

Table 2
Diagnostic performance of mm-wave dielectric measurements for breast tissue discrimination.

	AUC	Sensitivity	Specificity	PPV	NPV
MAL vs (FCD + NBT)	0.78 ± 0.03	0.869	0.574	0.131	0.426
MAL vs NBT	0.92 ± 0.02	0.930	0.860	0.070	0.140
FCD vs NBT	0.86 ± 0.02	0.850	0.796	0.150	0.204
MAL vs FCD	0.68 ± 0.05	0.775	0.589	0.025	0.411

findings (Figure 3b): MAL and FCD were both distinguished from NBT with high degrees of accuracy ($AUC_{MAL\ vs\ NBT}$: 0.92 ± 0.02; $AUC_{FCD\ vs\ NBT}$: 0.86 ± 0.02), whereas the distinction between MAL and FCD was clearly lower ($AUC_{MAL\ vs\ FCD}$: 0.68 ± 0.05).

4. Discussion

Our results extend previous reports of the potential for diagnostic use of tissue dielectric properties in discriminating breast lesions to the mm-wave frequencies. In particular, using a probe whose sensitivity profile adheres to recent guidelines on clear margin depth in conservative breast surgery and 5-fold cross-validation of a Bayesian logistic model for the tissue classification, our accuracy in distinguishing malignant from normal breast tissue was high (AUC 0.92), and good with respect to non-malignant tissues generally (AUC 0.78).

In evaluating a closely related approach to margin assessment, namely the radio-frequency-based MarginProbe® device, Kaufman et al. [26] have reported performing 4322 measurements on 106 samples. The differentiation between malignant lesions and fat-dominant mammary tissue was characterized by an ROC curve with AUC of 0.96, and sensitivity and specificity of 90 and 91% respectively. Our performance is very similar to these results for distinction between malignant and normal breast tissues (MAL vs NBT), though perhaps lower for malignant vs non-malignant tissues (MAL vs NBT + FCD). It should be noted however, that the performance in [26] is likely to be overestimated due to the non-independence of the samples following the large number of measurements replicated within each patient. Equally, the fraction of tissue samples in that study that did not correspond to malignant or healthy breast tissue (i.e. likely to be FCD) was far lower than in our sample cohort. Conversely, cross-validation as used our study may over-estimate performance due to over-fitting though we expect this to be very limited given the large differences seen in the Cole-Cole properties between the histopathological classes (Fig. 2). As the parallelepipeds of tissue prepared for our study were selected based on gross pathology assessment to contain a mixture of normal and abnormal tissue for each patient, it may also be that we have over-represented fibrocystic disease with a resultant reduction in the performance of distinguishing malignant vs non-malignant tissues (MAL vs NBT + FCD) This represents one of the principle limitations of our study. As a further note, Kaufman et al. [26] performed pathology assessment on a tissue plane parallel to the cut surface and thus may have underestimated the presence of malignant or fibrocystic tissues within the 2 mm margin thickness but outside the examined plane.

Operating at frequencies of 0.15–2.0 THz, considered the next band of frequencies higher than those used in the present work, Grootendorst et al. [18] have examined a small number of specimens evaluated reporting sensitivity, specificity, PPV and NPV with

a support vector machine classifier of 86%, 66%, 67% and 85%, respectively for the classification of malignant vs. benign tissues. Here, our performance matches in terms of sensitivity, but is substantially lower in PPV and NPV.

In contrast to our system and the MarginProbe® device [26], the system used by Grootendorst et al. [18] is optical in nature, using short laser pulses to achieve a depth resolution of 0.6 mm up to several millimetres below the tissue surface. Key issues for any surgical margin evaluation technique are spatial resolution, ability to cover the entire resection surface, time and cost-effectiveness. Given the early stage of the present work, it is difficult to comment on possible cost effectiveness of mm-wave margin evaluation. As regards spatial resolution and time, the device used in the present work provides an averaged response over a hemispherical volume of radius roughly ~3 mm and the acquisition per site requires a few seconds. This spatial resolution is limited relative to microscopy and suitably adapted conventional imaging approaches. As with microscopy and spectroscopy the present device requires translation over the excised tissue surface to provide a complete evaluation. A robotic approach, as has recently been demonstrated with a Raman spectroscopy system [41] is a possible strategy for avoiding handling difficulties. Accelerating the acquisition may be possible simultaneous multi-point measurements using an array of antennas as seen with the ClearEdge® device [13].

As seen previously at lower frequencies, we found two of the five parameters involved in the Cole-Cole model dielectric properties (e_s and σ_s) to be strongly correlated to fat content [11,12]. This likely explains the lower performance in distinguishing malignant from fibrocystic disease (AUC 0.68) as a high density of cells and interstitial fluid characterizes both and consequently a low fat content compared to normal breast tissue. To improve performance in this area, it is likely to be necessary to go beyond dielectric properties alone, and to incorporate additional independent information about the tissues. A number of options exist for doing so, including pre-operative mammography or ultrasound to provide densitometry characteristics of breast tissue, coupling the mmWave probe to a device for elastographic characterization of pseudotumoral sclerosing lesions of intra-operative use, or limiting gross intraoperative evaluation with or without frozen section analysis to these uncertain cases.

It remains to verify our findings in the intra-operative context, using fresh, ex-vivo breast tissue and comparison with the final histopathology findings on a per-resection basis both with and without intraoperative macroscopic assessment by a pathologist. Nonetheless, our experience leads to a couple of considerations for future developments. First, our finding of significant inter-patient variability in the Cole-Cole parameters due to the patients themselves (i.e. not related with the disease) has implications for the choice of statistical analysis applied to classification of tissues. Experimental designs in future should examine replicate sampling within subjects to control for among-subject variability in response to treatments before generalized results to patients beyond those involved the experiment. At the same time, the patient specific effect raises the possibility that diagnostic performance can be improved by adjusting the decision criteria on the basis of measurements on fatty tissues of the individual patient.

Second, despite a number of devices, putatively able to guide the surgeon during breast resection already being available so far, none of them has had a significant clinical or commercial impact. The system used in this study can be subjected to extreme simplification of electronics, which should allow the device to be cost-effective not only in hospitals that are not equipped to perform intraoperative pathology, but also in aiding a pathologist to choose the areas of interest to submit to the frozen section. The system allows assessment of individual points on a tissue surface in a few seconds and should Also to be examined is whether the sensitivity to pathology extends to surgical contexts beyond breast cancer.

In conclusion, we have demonstrated that the diagnostic potential of dielectric properties extends to the mm-wave frequencies using a system that adheres to recommendations for evaluation of surgical margins in breast cancer. Translation to use in evaluation of the surgical margin in breast conservation surgery will require validation of our results in the intra-operative setting, and the design of a low-cost device that allows rapid margin assessment while maintaining performance in discriminating tumor foci.

Ethical approval

This study was approved by the Ethical Committee for the IEO, European Institute of Oncology. All patients provided written informed consent for their participation in the study.

Conflicts of interest

Authors Bozzi, Matrone, Mazzanti, Pasian, Perregrini, Renne, Summers, and Svelto are co-inventors in a patent application related to this work.

Funding

This work was supported by AIRC, the Italian Association for Research into Cancer (Associazione Italiana per la Ricerca sul Cancro) [grant number: AIRC 13 - IG - Bellomi].

Acknowledgements

The authors would like to thank Cristiana Fodor for her assistance with the registering of patient consent and clinical study managment. The authors would also like to thank the members of the gross pathology team at IEO for their assistance in preparing samples for measurement.

Appendix A. Supplementary data

Supplementary data related to this article can be found at https://doi.org/10.1016/j.breast.2019.02.008.

References

[1] Veronesi U, Cascinelli N, Mariani L, et al. Twenty-year follow-up of a randomized study comparing breast-conserving surgery with radical mastectomy for early breast cancer. N. Engl. J. Med. 2002;347(16):1227–32. https://doi.org/10.1056/NEJMoa020989.

[2] de Alcantara Filho U, Capko D, Barry JM, Morrow M, Pusic A, Sacchini VS. Nipple-sparing mastectomy for breast cancer and risk-reducing surgery: the memorial sloan-Kettering cancer center experience. Ann Surg Oncol 2011;18(11):3117–22. https://doi.org/10.1245/s10434-011-1974-y.

[3] Pilewskie M, Morrow M. Margins in breast cancer: how much is enough? Cancer 2018;124(7):1335–41. https://doi.org/10.1002/cncr.31221.

[4] Dunne C, Burke JP, Morrow M, Kell MR. Effect of margin status on local recurrence after breast conservation and radiation therapy for ductal carcinoma in situ. J Clin Oncol 2009;27(10):1615–20. https://doi.org/10.1200/JCO.2008.17.5182.

[5] Marinovich ML, Azizi L, Macaskill P, et al. The association of surgical margins and local recurrence in women with ductal carcinoma in situ treated with breast-conserving therapy: a meta-analysis. Ann Surg Oncol 2016;23(12):3811–21. https://doi.org/10.1245/s10434-016-5446-2.

[6] Morrow M, Van Zee KJ, Solin LJ, et al. Society of surgical oncology-American society for radiation oncology - American society of clinical oncology consensus guideline on margins for breast-conserving surgery with whole-breast irradiation in ductal carcinoma in situ. J Clin Oncol 2016;34(33):4040–6. https://doi.org/10.1200/JCO.2016.68.3573.

[7] Jeevan R, Cromwell DA, Trivella M, et al. Reoperation rates after breast conserving surgery for breast cancer among women in England: retrospective study of hospital episode statistics. The BMJ 2012;345:e4505. https://doi.org/10.1136/bmj.e4505.

[8] McCahill LE, Single RM, Aiello Bowes EJ, et al. Variability in re-excision following breast conservation surgery. J Am Med Assoc 2012;307(5):467–75. https://doi.org/10.1001/jama.2012.43.
[9] Mulleniz PS, Cuadrado DG, Steele SR, et al. Secondary operations are frequently required to complete the surgical phase of therapy in the era of breast conservation and sentinel lymph node biopsy. Am J Surg 2004;187:643–6. https://doi.org/10.1016/j.amjsurg.2004.01.003.
[10] Balog J, Sasi-Szabó L, Kinross J, et al. Intraoperative tissue identification using rapid evaporative ionization mass spectrometry. Sci Transl Med 2013;5(194). https://doi.org/10.1126/scitranslmed.3005623. 194ra93–194ra93.
[11] Gabriel C, Gabriel S, Corthout E. The dielectric properties of biological tissues: I. Literature survey. Phys Med Biol 1996;41(11):2231–49. https://doi.org/10.1088/0031-9155/41/11/001.
[12] Lazebnik M, Popovic D, McCartney L, et al. A large-scale study of the ultrawideband microwave dielectric properties of normal, benign and malignant breast tissues obtained from cancer surgeries. Phys Med Biol 2007;52(20):6093–115. https://doi.org/10.1088/0031-9155/52/20/002.
[13] Dixon JM, Renshaw L, Young O, et al. Intra-operative assessment of excised breast tumour margins using ClearEdge imaging device. Eur J Surg Oncol 2016;42(7):1834–40. https://doi.org/10.1016/j.ejso.2016.07.141.
[14] Coble J, Reid V. Achieving clear margins. Directed shaving using MarginProbe, as compared to a full cavity shave approach. Am J Surg 2017;213(4):627–30. https://doi.org/10.1016/j.amjsurg.2016.12.019.
[15] Allweis TM, Kaufman Z, Lelcuk S, et al. A prospective, randomized, controlled, multicenter study of a real-time, intraoperative probe for positive margin detection in breast-conserving surgery. Am J Surg 2008;196(4):483–9. https://doi.org/10.1016/j.amjsurg.2008.06.024.
[16] Kupstas A, Ibrar W, Hayward RD, Ockner D, Wesen C, Falk J. A novel modality for intraoperative margin assessment and its impact on re-excision rates in breast conserving surgery. Am J Surg 2018;215(3):400–3. https://doi.org/10.1016/j.amjsurg.2017.11.023.
[17] Schnabel F, Boolbol SK, Gittleman M, et al. A randomized prospective study of lumpectomy margin assessment with use of MarginProbe in patients with nonpalpable breast malignancies. Ann Surg Oncol 2014;21(5):1589–95. https://doi.org/10.1245/s10434-014-3602-0.
[18] Grootendorst MR, Fitzgerald AJ, Brouwer de Koning SG, et al. Use of a handheld terahertz pulsed imaging device to differentiate benign and malignant breast tissue. Biomed Opt Express 2017;8:2932–45. https://doi.org/10.1364/BOE.8.002932.
[19] Ha R, Friedlander LC, Hibshoosh H, et al. Optical coherence tomography: a novel imaging method for post-lumpectomy breast margin assessment-A multi-reader study. Acad Radiol 2018;25(3):279–87. https://doi.org/10.1016/j.acra.2017.09.018.
[20] McClatchy 3rd DM, Zuurbier RA, Wells WA, Paulsen KD, Pogue BW. Micro-computed tomography enables rapid surgical margin assessment during breast conserving surgery (BCS): correlation of whole BCS micro-CT readings to final histopathology. Breast Canc Res Treat 2018;172(3):587–95. https://doi.org/10.1007/s10549-018-4951-3.
[21] Pop MM, Cristian S, Hanko-Bauer O, Ghiga DV, Georgescu R. Obtaining adequate surgical margin status in breast-conservation therapy: intraoperative ultrasound-guided resection versus specimen mammography. Cluj Med 2018;91(2):197–202. https://doi.org/10.15386/cjmed-891.
[22] Papa M, Allweis T, Karni T, et al. An intraoperative MRI system for margin assessment in breast conserving surgery: initial results from a novel technique. J Surg Oncol 2016 Jul;114(1):22–6. https://doi.org/10.1002/jso.24246.
[23] Brachtel EF, Johnson NB, Huck AE, et al. Spectrally encoded confocal microscopy for diagnosing breast cancer in excision and margin specimens. Lab Invest 2016;96(4):459–67. https://doi.org/10.1038/labinvest.2015.158.
[24] Yoshitake T, Giacomelli MG, Quintana LM, et al. Rapid histopathological imaging of skin and breast cancer surgical specimens using immersion microscopy with ultraviolet surface excitation. Sci Rep 2018;8(1):4476. https://doi.org/10.1038/s41598-018-22264-2.
[25] Giacomelli MG, Yoshitake T, Cahill LC, et al. Multiscale nonlinear microscopy and widefield white light imaging enables rapid histological imaging of surgical specimen margins. Biomed Opt Express 2018;9(5):2457–75. https://doi.org/10.1364/BOE.9.002457.
[26] Kaufman Z, Paran H, Haas I, et al. Mapping breast tissue types by miniature radio-frequency near-field spectroscopy sensor in ex-vivo freshly excised specimens. BMC Med Imaging 2016;16:57. https://doi.org/10.1186/s12880-016-0160-x.
[27] Birtoiu IA, Rizea C, Togoe D, et al. Diagnosing clean margins through Raman spectroscopy in human and animal mammary tumour surgery: a short review. Interface Focus 2016;6(6):20160067. https://doi.org/10.1098/rsfs.2016.0067.
[28] de Boer LL, Molenkamp BG, Bydlon TM, et al. Fat/water ratios measured with diffuse reflectance spectroscopy to detect breast tumor boundaries. Breast Canc Res Treat 2015;152(3):509–18. https://doi.org/10.1007/s10549-015-3487-z.
[29] Phipps JE, Gorpas D, Unger J, Darrow M, Bold RJ, Marcu L. Automated detection of breast cancer in resected specimens with fluorescence lifetime imaging. Phys Med Biol 2017;63(1):015003. https://doi.org/10.1088/1361-6560/aa983a.
[30] Shipp DW, Rakha EA, Koloydenko AA, Macmillan RD, Ellis IO, Notingher I. Intra-operative spectroscopic assessment of surgical margins during breast conserving surgery. Breast Cancer Res 2018;20(1):69. https://doi.org/10.1186/s13058-018-1002-2.
[31] Allen WM, Chin L, Wijesinghe P, et al. Wide-field optical coherence microelastography for intraoperative assessment of human breast cancer margins. Biomed Opt Express 2016;7(10):4139–53. https://doi.org/10.1364/BOE.7.004139.
[32] Wong TTW, Zhang R, Hai P, et al. Fast label-free multilayered histology-like imaging of human breast cancer by photoacoustic microscopy. Sci Adv 2017;3(5):e1602168. https://doi.org/10.1126/sciadv.1602168.
[33] Dintzis SM, Hansen S, Harrington KM, et al. Real-time visualization of breast carcinoma in pathology specimens from patients receiving fluorescent tumor-marking agent tozuleristide. Arch Pathol Lab Med 2018 Dec 14. https://doi.org/10.5858/arpa.2018-0197-OA.
[34] Preece AW, Craddock I, Shere M, Jones L, Winton HL. MARIA M4: clinical evaluation of a prototype ultrawideband radar scanner for breast cancer detection. J Med Imaging 2016;3(3):033502. https://doi.org/10.1117/1.JMI.3.3.033502.
[35] Bourqui J, Zarnke SM, Budzis JR, Garrett DC, Mew DJY, Fear EC. Bulk permittivity variations in the human breast over the menstrual cycle. 11th european conference on antennas and propagation. EUCAP); 2017. p. 3476–9. https://doi.org/10.23919/EuCAP.2017.7928600.
[36] Marsland TP, Evans S. Dielectric measurements with an open-ended coaxial probe. IEE Proc H Microwaves, Antennas Propag 1987;134(4):341–9. https://doi.org/10.1049/ip-h-2.1987.0068.
[37] Martellosio A, Pasian M, Bozzi M, et al. Dielectric properties characterization from 0.5 to 50 GHz of breast cancer tissues. IEEE Trans Microw Theory Tech 2017;65(3):998–1011. https://doi.org/10.1109/TMTT.2016.2631162.
[38] Yamaguchi R, Tsuchiya S, Koshikawa T, et al. Evaluation of inadequate, indeterminate, false-negative and false-positive cases in cytological examination for breast cancer according to histological type. Diagn Pathol 2012;7:53. https://doi.org/10.1186/1746-1596-7-53.
[39] R Core Team. R. A language and environment for statistical computing. Vienna, Austria: R Foundation for Statistical Computing; 2015. https://www.R-project.org/. [Accessed 20 September 2018].
[40] Jarrod D, Hadfield H. MCMC methods for multi-response generalized linear mixed models: the MCMCglmm R package. J Stat Software 2010;33(2):1–22. https://doi.org/10.18637/jss.v033.i02.
[41] Thomas G, Nguyen T-Q, Pence IJ, et al. Evaluating feasibility of an automated 3-dimensional scanner using Raman spectroscopy for intraoperative breast margin assessment. Sci Rep 2017;7:13548. https://doi.org/10.1038/s41598-017-13237-y.